# $K$ x-ray production cross sections for fourteen elements from calcium to palladium for incident carbon ions*

R. M. Wheeler and R. P. Chaturvedi
*State University of New York College, Cortland, New York 13045*

J. L. Duggan and J. Tricomi
*North Texas State University,† Denton, Texas 76201*

P. D. Miller
*Oak Ridge National Laboratory, Oak Ridge, Tennessee 37830*
(Received 18 February 1975; revised manuscript received 8 October 1975)

Absolute $K$-shell x-ray production cross sections for thin Ca, Sc, Ti, V, Fe, Ni, Cu, Zn, Ge, Rb, Sr, Y, Zr, and Pd targets have been measured for incident carbon ions in the energy range from 8 to 36 MeV. Ionization cross sections are calculated from atomic $K$-shell fluorescence yields and compared to the theoretical predictions of the plane-wave Born approximation including binding energy, Coulomb deflection, and relativistic corrections. $K\alpha/K\beta$ ratios and the shifts in the characteristic $K\alpha$ and $K\beta$ energies indicate the existence of multiple ionization in the low-$Z$ targets.

## I. INTRODUCTION

Garcia *et al.*,[1] Richard,[2] and Saris[3] have summarized up-to-date experimental results of heavy-ion–atom collisions. From a survey of these papers it is found that no systematic study of x-ray production cross sections has been made with carbon ions. Recently Hansen *et al.*[4] and Li and Watson[5] have studied $K\alpha/K\beta$ intensity ratios for x-ray production by carbon ions and compared them with those for fast deuterons and $\alpha$ particles.

The purpose of this work has been (i) to measure $K$ x-ray production cross sections for fourteen elements with atomic numbers in the range $20 \leq Z \leq 46$ for incident carbon ions with energies from 8 to 36 MeV, (ii) to compare these results with the plane-wave Born approximation (PWBA) calculations of Basbas *et al.*[6] which include corrections for binding energy and Coulomb deflection effects, and (iii) to examine $K\alpha/K\beta$ ratios and shifts of the characteristic x-ray energies of the target atoms.

## II. EXPERIMENTAL PROCEDURE

Carbon ions in charge states from 2+ to 5+ were accelerated to the energy range 8–36 MeV by the Oak Ridge National Laboratory EN tandem Van de Graaff accelerator. The characteristic x-ray spectra of calcium ($Z=20$), scandium ($Z=21$), titanium ($Z=22$), vanadium ($Z=23$), iron ($Z=26$), nickel ($Z=28$), copper ($Z=29$), zinc ($Z=30$), germanium ($Z=32$), rubidium ($Z=37$), strontium ($Z=38$), yttrium ($Z=39$), zirconium ($Z=40$), and palladium ($Z=46$) were obtained as a function of energy.

The carbon ions passed through two tantalum apertures, which collimated the beam of ions to a diameter of 2 mm on target, and then into a Faraday cup. A rotatable target holder allowed 24 targets to be mounted in the vacuum chamber and bombarded individually.[7] X rays from a given target were detected by a Si(Li) detector (0.000 85-cm Be window, active area 38 mm$^2$) subtending a fractional solid angle of $4.0 \times 10^{-4}$. The Si(Li) detector was mounted directly in the vacuum chamber with an O-ring seal. A 0.45-mm Mylar foil was placed between the target and the Si(Li) detector to eliminate low-energy background radiation produced primarily by secondary-electron bremsstrahlung emission. The efficiency–solid-angle product $\epsilon_f$ and the energy calibration of the detection system for measuring x rays were determined by positioning calibrated x-ray sources at the same position as the beam spot on target. The calibrated sources, $^{51}$Cr, $^{55}$Fe, $^{57}$Co, $^{65}$Zn, and $^{241}$Am, yielded 12 different points for efficiency and energy calibration curves in the energy range 3.35–26.35 keV. Efficiencies in this energy range were obtained from a fourth-order polynomial fit to the calibration points as a function of energy. The stability of the energy calibration was checked frequently by monitoring $^{57}$Co spectra between cross-section measurements. Over the course of the experiment the variation in the position of the $^{57}$Co $K$ x rays was on the order of 10 eV, which is the estimated accuracy of the energy-shift data.

The total number of incident carbon ions was determined from the number forward scattered into a surface barrier detector mounted at an angle of 30° with respect to the beam axis. For the elements and energies studied in this work both nuclear deviations from Rutherford scattering and atomic screening effects are negligible.[8,9] The surface barrier detector subtended a solid angle of $8.15\times10^{-4}$ sr.

The targets were made by vacuum deposition of high-purity elements on 5–20 $\mu$g/cm$^2$ carbon foils supported by aluminum target frames. The target thicknesses ranged from 5 to 20 $\mu$g/cm$^2$ and were sufficiently thin to allow us to neglect degradation of the incident carbon-ion energy as well as self-absorption of the emitted characteristic x rays in the targets.

The amplified detector outputs of both x-ray and charged-particle detectors were each stored in 1000 channels of a 16 000 channel analyzer which was multiplexed to a PDP-11 and a CDC 3200 computer for plotting and data reduction by light-pen stripping. The dead times in both data channels were generally kept below 5%.

Characteristic x-ray energies were determined from the centroids of the observed x-ray peaks and the aforementioned energy calibration. Energy shifts were taken as the difference between the measured x-ray energies and those for single $K$-shell ionization given by Bearden and Burr.[10]

## III. RESULTS AND DISCUSSION

The $K$ x-ray production cross section $\sigma_x$ is given by

$$\sigma_x = \frac{(N_\alpha/\epsilon_\alpha + N_\beta/\epsilon_\beta)}{N_c}\frac{d\sigma_R}{d\Omega}\Delta\Omega ,$$

where $N_\alpha$ and $N_\beta$ are the number of $K\alpha$ and $K\beta$ x rays detected in the Si(Li) detector with total efficiency–solid-angle products $\epsilon_\alpha$ and $\epsilon_\beta$, respectively; $N_c$ is the number of carbon ions scattered into the surface barrier detector subtending a solid angle $\Delta\Omega$, and $d\sigma_R/d\Omega$ is the Rutherford differential scattering cross section. The measured $K$ x-ray production cross sections are given in Table I as a function of carbon-ion energy along with estimated errors and incident-ion charge state. The main sources of error were the uncertainty in the efficiency–solid-angle product of the x-ray detector and statistics.

The calculation of ionization cross sections, given as $\sigma_K=\sigma_x/\omega_K$, from the measured x-ray production cross sections creates some problems since the fluorescence yield $\omega_K$ for heavy-ion induced ionization varies with the amount of multiple ionization. However, in order to compare with the theoretical ionization predictions, the following best-fit values for $\omega_K$, taken from the paper by Bambynek *et al.*,[11] were used: for Ca, 0.163; Sc, 0.190; Ti, 0.219; V, 0.250; Fe, 0.347; Ni, 0.414; Cu, 0.445; Zn, 0.479; Ge, 0.540; Rb, 0.669; Sr, 0.691; Y, 0.711; Zr, 0.730; and Pd, 0.819.

TABLE I. $K$-shell x-ray production cross sections for $^{12}$C ion bombardment at energies from 8 to 36 MeV. All cross sections are in b. Footnotes give the error in the cross-section measurements.

| Elem. \ $E_c$ (MeV) / Ion | 8<br>$2^+$ | 11<br>$3^+$ | 12<br>$3^+$ | 14<br>$4^+$ | 16<br>$3^+$ | 17<br>$4^+$ | 20<br>$4^+$ | 22.75<br>$4^+$ | 24<br>$4^+$ | 26<br>$4^+$ | 28<br>$4^+$ | 29<br>$4^+$ | 32<br>$5^+$ | 36<br>$5^+$ |
|---|---|---|---|---|---|---|---|---|---|---|---|---|---|---|
| Ca [a] | 260 | 1400 | 1400 | 3400 | ··· | 6700 | 8800 | 14 000 | 16 000 | 18 000 | 20 000 | 23 000 | 31 000 | 34 000 |
| Sc [b] | ··· | 600 | ··· | 1500 | ··· | 3700 | 5200 | 8200 | ··· | 12 000 | ··· | ··· | 20 000 | ··· |
| Ti [c] | 110 | ··· | 590 | 1200 | ··· | ··· | 4400 | 7000 | 7800 | 10 000 | 11 000 | ··· | 15 000 | 16 000 |
| V [d] | 77 | ··· | 390 | ··· | 1600 | ··· | 2800 | ··· | 5700 | ··· | 8600 | ··· | 12 000 | 14 000 |
| Fe [e] | 32 | ··· | 140 | ··· | 480 | ··· | 1100 | ··· | 2000 | ··· | 3500 | ··· | 5600 | 6800 |
| Ni [d] | 17 | 46 | 69 | 110 | 220 | 280 | 510 | ··· | 1200 | ··· | 1900 | ··· | 3000 | 3400 |
| Cu [d] | 12 | ··· | 51 | ··· | ··· | ··· | 380 | ··· | 900 | ··· | 1500 | ··· | 2300 | 2600 |
| Zn [e] | 9.3 | ··· | 37 | ··· | 120 | ··· | 250 | ··· | 620 | ··· | 1100 | ··· | 1600 | 2100 |
| Ge [e] | 5.0 | ··· | 24 | ··· | 63 | ··· | 140 | ··· | 320 | ··· | 530 | ··· | 760 | 1100 |
| Rb [d] | 1.5 | ··· | 6.5 | ··· | 19 | ··· | 36 | 63 | 72 | ··· | 130 | ··· | 220 | 300 |
| Sr [c] | ··· | 4.1 | ··· | 8.8 | ··· | 18 | 32 | 47 | ··· | 83 | ··· | 120 | 170 | ··· |
| Y [e] | 1.2 | 3.5 | 4.6 | 7.5 | ··· | 15 | 25 | 40 | 49 | 65 | ··· | 110 | 150 | 190 |
| Zr [e] | 1.0 | ··· | 3.8 | ··· | 11 | ··· | 21 | ··· | 46 | ··· | 72 | ··· | 110 | 160 |
| Pd [c] | 0.34 | 0.90 | 1.3 | 2.0 | ··· | 4.1 | 7.3 | 11 | 13 | 18 | ··· | 27 | 38 | 46 |

[a] ±25%
[b] ±20%
[c] ±15%
[d] ±12%
[e] ±10%

In Fig. 1 the $K$-shell ionization cross sections inferred from the data are plotted for comparative purposes as scaled cross sections, $\theta_K\sigma_K/\sigma_{0K}$, as a function of scaled projectile energy $\eta_K/\theta_K^2$, where $\theta_K = U_K/Z_2^2 R$ is a screening number which measures the nonhydrogenic behavior of the $K$-shell ionization energy $U_K$ ($R = 13.6$ eV), $\sigma_{0K} = 8\pi a_0^2 Z_1^2/Z_2^4$ is a wave-mechanical cross section for the two $K$ electrons weighted by the square of the scaled Coulomb-interaction strength (subscripts 1 and 2 refer to the projectile and target atom, respectively, and $a_0 = 0.529$ Å), and $\eta_K = v_1^2/v_{2K}^2$ is the square of the ratio of the projectile velocity to the mean $K$-shell velocity, where $v_{2K} = Z_2 v_0$ ($v_0 = 2.19 \times 10^8$ cm/sec). In this representation the PWBA predictions form a universal curve. One finds in Fig. 1 that at low projectile velocities the experimental results are considerably lower than the predicted theoretical values while at the highest projectile velocities the theoretical predictions fall below the experimental values. The figure also indicates that at the lower energies the cross sections for the lighter target elements deviate from the theory more than do the heavier target elements.

Deviations from the simple PWBA have been observed and discussed by numerous authors in the past few years. At projectile velocities that are low compared to the $K$-shell electron velocities the cross sections are reduced owing to the increased binding energy of the $K$ electrons when a projectile has an impact parameter that is small compared to the $K$-shell Bohr radius and from Coulomb deflection of the projectile. Corrections for Coulomb deflection are included in later versions of the binary-encounter-approximation (BEA) formulations of the ionization process[12,13] and both increased binding and Coulomb deflection have been applied as perturbations to the PWBA for $K$- and $L$-shell[6,14] ionization. At higher energies, when projectile velocities are comparable to $K$-shell electron velocities, the cross sections are increased owing to polarization of the $K$ electron shell by the projectile and possible charge exchange with the projectile. Theoretical corrections for these effects are not available as yet.

As noted before, multiple ionization could also cause an apparent increase in ionization cross sections inferred from x-ray production measurements owing to increases in the fluorescence yields. Except for a very few specific elements, calculations for fluorescence yield as a function of multiple ionization are not available. However, for the present data, the discrepancies are estimated to be no higher than 30% in calcium, 10%, in zinc, and negligible in palladium.[15]

The effects due to increased binding energy and Coulomb deflection calculated by Basbas *et al.*[6] have been applied to the PWBA theory and to the data and are shown in Fig. 2. The PWBA scaling parameters are the same as described before with

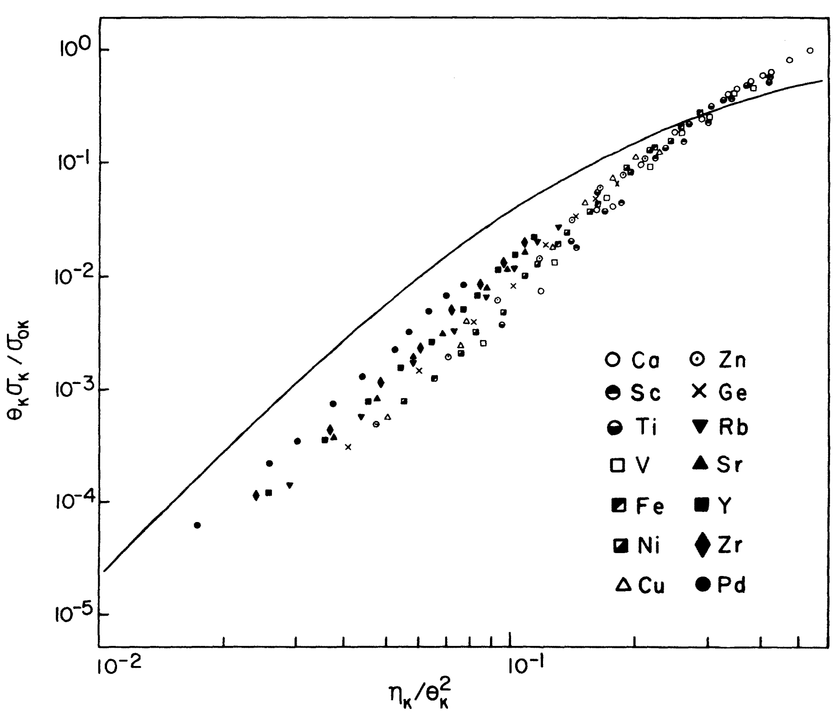


FIG. 1. Universal plot of $K$-shell ionization cross sections for carbon ions on Ca, Sc, Ti, V, Fe, Ni, Cu, Zn, Ge, Rb, Sr, Y, Zr, and Pd. In this representation the PWBA is given by a universal curve (Table V of Ref. 6).

two exceptions: (i) The effect of a Coulomb deflection factor has been divided out of the experimental cross sections since it destroys the universal scaling of the theory. This factor is defined in Eq. (33a) of Basbas *et al.*[6] and is given by $f_c = 9E_{10}(\pi d q_0)$. (ii) The increase in binding energy is reflected by an increase in the screening number by the factor $\epsilon$ [$\epsilon$ is defined in Eqs. (37) and (39) of Basbas *et al.*[6]]. As seen in Fig. 2 the corrections have caused the data to coalesce to a more universal pattern, although now everywhere greater than the PWBA.

A further improvement of the fit of the data to the PWBA, especially for the higher-$Z$ elements, can be made by considering relativistic effects. While no exact theoretical treatment of relativistic effects is available (except for the works of Jamnik and Zupancic,[16] Choi,[17] and Miller[18]) Merzbacher and Lewis[19] (following a procedure developed by Hönl[20]) and Hardt and Watson[21] have used semirelativistic methods to calculate effective changes in the scaled energy, independent of the projectile bombarding energy, owing to the relativistic velocity of the $K$-shell electrons. Hansen,[13] in a configuration-space treatment of the BEA, sets

$$m = m_e(1 + v_2^2/2c^2),$$

where the $K$-shell electron velocity $v_2$ is a function of the impact parameter. This approach produces increasing corrections for decreasing projectile energies, which is consistent with the observation that in Fig. 2 for $\eta_K/(\epsilon\theta_K)^2 < 0.05$ the deviations of the cross sections from the universal PWBA curve are increasing as energy decreases. With the use of an addendum[22] to Hansen's paper which gives the ratio of relativistic to nonrelativistic BEA cross sections, $f_R$, as a function of $E_1/\lambda U_K$ ($\lambda = M_1/m_e$) and $Z_2$, we have interpolated (or extrapolated for $E_1/\lambda U_K \le 0.027$) values of $f_R$ for each element having an effective charge $Z_2^{\mathrm{eff}} = \epsilon^{1/2} Z_2$ and effective binding energy $U_K^{\mathrm{eff}} = \epsilon U_K$, as a function of $E_1/\lambda U_K^{\mathrm{eff}}$. This ratio has been divided into the data[23] and the results are given in Fig. 3, with all other parameters being the same as in Fig. 2.

With the addition of the relativistic corrections there is reasonably good agreement between the data and the PWBA with corrections for $\eta_K/(\epsilon\theta_K)^2 < 0.05$. Above this point the data begin to diverge from the PWBA. On the assumption that this deviation is due primarily to positive $(Z_1/Z_2\theta_K)^3$ effects (polarization) we have plotted in Fig. 4 the difference between experiment and theory (including binding energy, Coulomb deflection, and relativistic corrections) times $(Z_2\theta_K/Z_1)^3$ as a function of $\eta_K/\theta_K^2$ for six elements. The good agreement for all elements indicates that inclusion of the positive $(Z_1/Z_2\theta_K)^3$ effect into the PWBA would account for a significant amount of the deviations from experiment apparent in Fig. 3. At the same

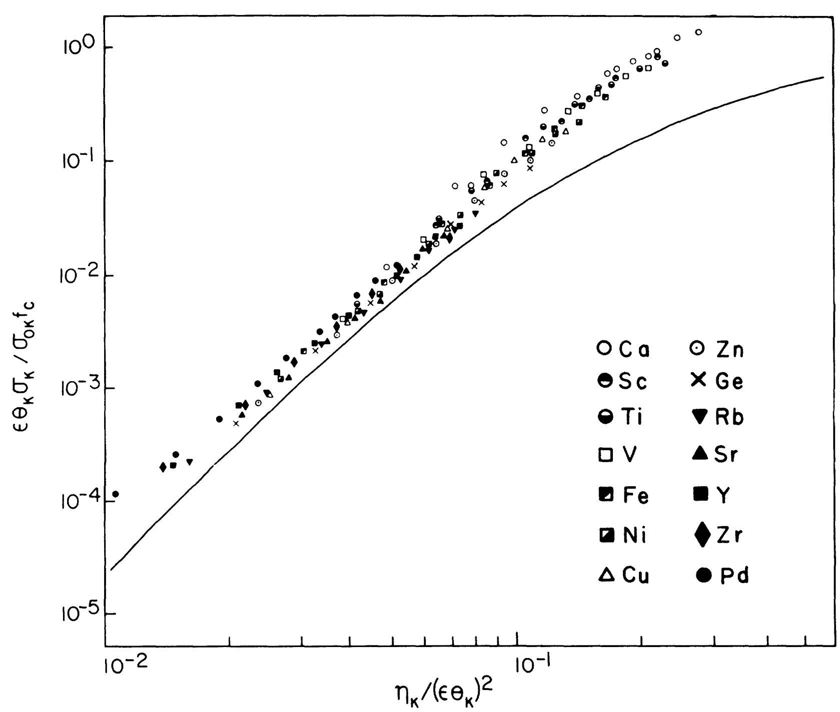


FIG. 2. Universal plot of $K$-shell ionization cross sections divided by a Coulomb-deflection correction factor $f_c$ and with $\theta_K$ replaced by an effective screening number $\epsilon\theta_K$.

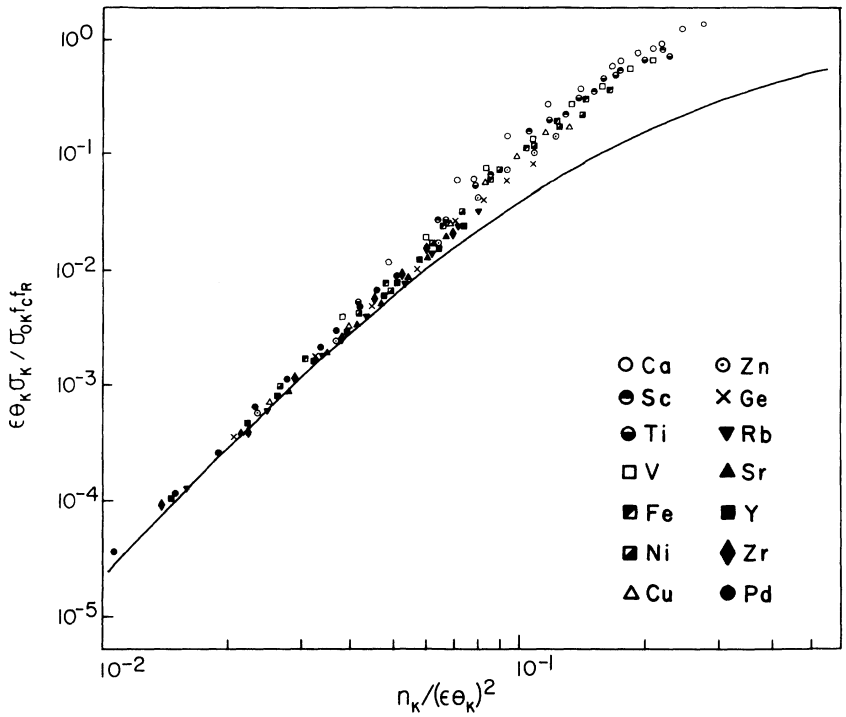


FIG. 3. Universal plot of $K$-shell ionization cross sections All parameters the same as in Fig. 2 with the exception that the experimental cross sections are divided by a relativistic correction calculated from Ref. 22.

time it appears likely that affects due to multiple ionization and charge exchange are small (<30%) and difficult to distinguish within the accuracy of the present experiment.

The values of $K\alpha/K\beta$ for the elements studied do not appear to change significantly as a function of energy. Representative values are given in Table II at 28 MeV and are compared to those of Li and Watson[5] at the same energy and to the calculated values of Scofield.[24] From Table II one sees that the low-$Z$ $K\alpha/K\beta$ data are suppressed with respect to the theoretical values. This is an indication of multiple ionization in the target $L$ shell.

The effects of multiple ionization are also reflected by the shifts in the characteristic energies of $K\alpha$ and $K\beta$ x rays. One expects the maximum energy shift to occur at the point where the incident projectile velocity matches the average velocity of the $L$-shell electrons, i.e., when $E_1/\lambda\bar{U}_L = 1$; however, the maximum energy shifts for Ca, Ti, Fe, and Zn occur at approximately $E_1/\lambda\bar{U}_L = 2.0$, 1.6, 1.4, and 1.0, respectively. This is explained by the fact that ionization takes place inside the $L$-shell Bohr radius and thus the effective average $L$-shell binding energy is greater than $\bar{U}_L$. Brandt and Lapicki[14] have recently published theoretical calculations which can be used to determine the increase in binding energy of each $L$

TABLE II. $K\alpha/K\beta$ for 28-MeV carbon ions with comparative values from Li and Watson (Ref. 5) and the theoretical values of Scofield (Ref. 24).

| | Ca | Sc | Ti | V | Fe |
|---|---|---|---|---|---|
| Present work [a] | 7.1 | ··· | 6.5 | 6.0 | 5.9 |
| Li and Watson | 5.71 ± 0.24 | 5.95±0.22 | 6.18 ± 0.27 | 6.42 ± 0.25 | 6.54 ± 0.17 |
| Scofield | 7.62 | ··· | 7.38 | 7.32 | 7.20 |

| | Ni | Cu | Zn | Ge | Rb | Zr |
|---|---|---|---|---|---|---|
| Present work [a] | 5.8 | 5.9 | 5.7 | 5.7 | 5.2 | 4.6 |
| Li and Watson | 6.173 ± 0.15 | 6.061 ± 0.18 | 6.098 ± 0.14 | 5.814 ± 0.15 | ··· | ··· |
| Scofield | 7.14 | 7.25 | 7.09 | 6.65 | 5.61 | 5.23 |

[a] Error: 5%.

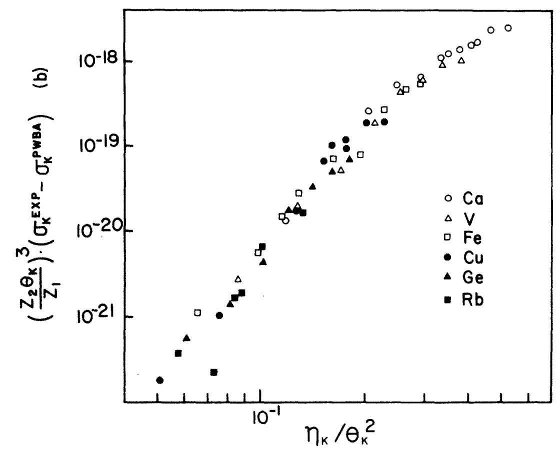


FIG. 4. Plot of the difference between experimental and corrected PWBA cross sections times $(Z_2\theta_K/Z_1)^3$.

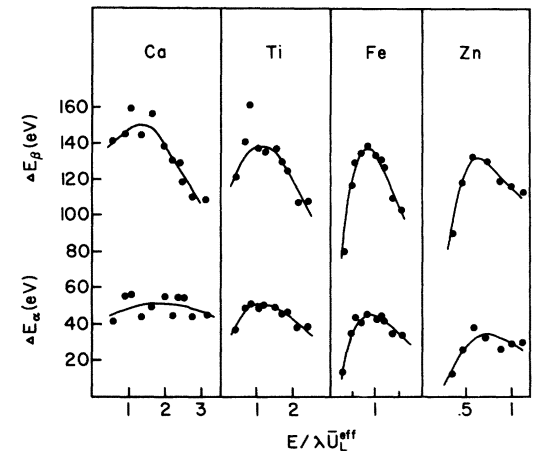


FIG. 5. Shifts in the characteristic energies of $K\alpha$ and $K\beta$ x rays of Ca, Ti, Fe, and Zn in terms of $E_1/\lambda\bar{U}_L^{\text{eff}}$. The lines through the data points are not theoretical fits but are drawn to help visualize the results.

subshell, $\epsilon_{L_i}$. Using this technique an effective average $L$-shell binding energy is calculated as

$$\bar{U}_L^{\text{eff}} = \tfrac{1}{4}(\epsilon_{L_1}U_{L_1} + \epsilon_{L_2}U_{L_2} + 2\epsilon_{L_3}U_{L_3}) .$$

The shifts in energy for Ca, Ti, Fe, and Zn as a function of $E_1/\lambda\bar{U}_L^{\text{eff}}$ are shown in Fig. 5, where the lines through the data are drawn to aid the eye. The maximum energy shifts occur at approximately $E_1/\lambda\bar{U}_L^{\text{eff}} = 1.2$, 1.1, 0.9, and 0.6 for Ca, Ti, Fe, and Zn, respectively. Thus these corrections tend to produce a more universal behavior of the data although there still appears to be some $Z_2$ dependence to the data. Using the atomic-structure-calculation tables of Herman and Skillman,[25] one finds that the average energy shifts in eV per $L$-shell vacancy for $K\alpha$ and $K\beta$ lines, respectively, are, for Ca, 20, 51; Ti, 23, 57; Fe, 30, 69; and Zn, 37, 82. Thus the $K$ x-ray energy shifts induced by carbon ions correspond to approximately two $L$-shell vacancies in Ca and to approximately one $L$-shell vacancy in Zn.

## IV. CONCLUSIONS

In summary, we conclude that the measured $K$-shell x-ray production cross sections for incident carbon ions are fairly well explained by the PWBA with corrections for Coulomb deflection, increased binding, and relativistic electron velocities where $\eta_K/(\epsilon\theta_K)^2 \lesssim 0.05$. Above this value the data begin to diverge from the PWBA with a dependence on atomic number suggesting a positive $(Z_1/Z_2\theta_K)^3$ effect. Within the limitations of experimental error, no dramatic increases in the fluorescence yields owing to multiple ionization can be inferred from the data. However, the presence of multiple ionization is indicated by the energy shifts and decreases in $K\alpha/K\beta$ ratios of the characteristic x-ray lines.

## ACKNOWLEDGMENTS

The authors would like to express their thanks to the Atomic Energy Commission for financial assistance in travel and lodging while this research was being undertaken, which was administered by Oak Ridge Associated Universities. We are also indebted to Ed Robinson, Jung Lin, George Pepper, and Bob Carlton for help in taking data and in computations. One of the authors (R.M.W.) would also like to thank Werner Brandt, C. P. Bhalla, and J. S. Hansen for useful conversations.

---

*Research supported in part by the Energy Research and Development Administration under contract with Union Carbide Corporation.

†Research supported by the Research Corporation and the North Texas State University Faculty Research Fund.

[1]J. D. Garcia, R. J. Fortner, and T. M. Kavanagh, Rev. Mod. Phys. 45, 111 (1973).

[2]P. Richard, in *Proceedings of the International Conference on Inner-Shell Ionization Phenomena, Atlanta, Georgia, 1972*, edited by R. W. Fink, S. T. Manson, J. M. Palms, and P. V. Rao, CONF-720 404 (U. S. Atomic Energy Commission, Oak Ridge, Tenn., 1973).

[3]F. W. Saris, *The Physics of Electron and Atomic Col-*

*lisions,* edited by T. R. Grover and F. J. de Heer (North-Holland, Amsterdam, 1972), p. 181.

[4]J. S. Hansen, T. K. Li, and R. L. Watson, in Ref. 2.

[5]T. K. Li and R. L. Watson, Phys. Rev. A 9, 1574 (1974).

[6]G. Basbas, W. Brandt, and R. Laubert, Phys. Rev. A 7, 983 (1973).

[7]Details of this chamber will be described in a later publication.

[8]A. W. Obst, D. L. McShan, and R. H. Davis, Phys. Rev. C 6, 1814 (1972), and private communication.

[9]E. Everhart, G. Stone, and R. J. Carbone, Phys. Rev. 99, 1287 (1955).

[10]J. A. Bearden and A. F. Burr, Rev. Mod. Phys. 39, 78 (1967).

[11]W. Bambynek, B. Crasemann, R. W. Fink, H. U. Freund, H. Mark, C. D. Swift, R. E. Price, and P. V. Rao, Rev. Mod. Phys. 44, 716 (1972).

[12]B. K. Thomas and J. D. Garcia, Phys. Rev. 179, 94 (1969).

[13]J. S. Hansen, Phys. Rev. A 8, 822 (1973).

[14]W. Brandt and G. Lapicki, Phys. Rev. A 10, 474 (1974).

[15]C. P. Bhalla (private communication).

[16]D. Jamnik and C. Zupancic, K. Dan. Vidensk. Selsk. Mat.-Fys. Medd. 31, 2 (1957).

[17]B.-H. Choi, Phys. Rev. A 4, 1002 (1971).

[18]P. D. Miller, Masters thesis (Rice University, 1956) (unpublished).

[19]E. Merzbacher and H. W. Lewis, Handb. Phys. 34, 166 (1955).

[20]H. Hönl, Z. Phys. 84, 1 (1933).

[21]T. L. Hardt and R. L. Watson, Phys. Rev. A 7, 1917 (1973).

[22]Addendum 1 to Ref. 13, unpublished. It should be noted that the table in the addendum is not only more comprehensive than the corresponding Table II given in Ref. 13 but also has slightly larger values.

[23]Although the nonrelativistic BEA and PWBA predictions are not equal, the energy dependence of both Hansen's nonrelativistic BEA and the PWBA with Coulomb-deflection corrections are similar in the energy region studied here. Thus the use of $f_R$ in the PWBA representation in Fig. 3 is not deemed unreasonable. A useful approximation inferred from Hansen's addendum (Ref. 22) is that if $f_R$ is written as $f_R = 1 + \zeta$, $\zeta = 2.675 \times 10^{-4} U_K^{\text{eff}} (E_1/\lambda U_K^{\text{eff}})^{-1.25}$ in the range $0.025 \leq E_1/\lambda U_K^{\text{eff}} \leq 1$ with an error in $f_R$ of less than 5%.

[24]J. H. Scofield, Phys. Rev. A 9, 1041 (1974).

[25]F. Herman and S. Skillman, *Atomic Structure Calculations* (Prentice-Hall, Englewood Cliffs, N. J., 1963).